ISSN 1063-7788, Physics of Atomic Nuclei, 2023, Vol. 86, No. 4, pp. 483–488. © Pleiades Publishing, Ltd., 2023.

ELEMENTARY PARTICLES AND FIELDS
Experiment

Detection of TeV Emission from the Crab Nebula Using the First Two IACTs in TAIGA in Stereo Mode of Observation

P. A. Volchugov[1),2)*, I. I. Astapov[3), P. A. Bezyazeekov[2), E. A. Bonvech[1), A. Borodin[4), N. Budnev[2), A. V. Bulan[1), A. Chiavassa[5), D. V. Chernov[1), A. Dyachok[2), A. Gafarov[2), A. Garmash[6),7), V. Grebenyuk[4),8), O. Gress[2), E. Gress[2), T. Gress[2), A. Grinyuk[4), O. Grishin[2), A. D. Ivanova[2), A. L. Ivanova[7),2), M. Ilushin[2), N. Kalmykov[1), V. Kindin[3), S. Kiryuhin[2), R. Kokoulin[3), N. Kolosov[2), K. Kompaniets[3), E. Korosteleva[1), V. Kozhin[1), E. Kravchenko[6),7), A. Kryukov[1), L. Kuzmichev[1), A. Lagutin[9), M. Lavrova[4), Y. E. Lemeshev[2), B. Lubsandorzhiev[10), N. Lubsandorzhiev[1), S. D. Malakhov[2), R. Mirgazov[2), R. Monkhoev[2), E. Osipova[1), E. Okuneva[1), A. Pakhorukov[2), A. Pan[3), L. Pankov[2), A. D. Panov[1), A. Petrukhin[3), D. A. Podgrudkov[1), E. Popova[1), E. Postnikov[1), V. Prosin[1), V. Ptuskin[11), A. Pushnin[2), R. Raikin[9), A. Y. Razumov[1), G. Rubtsov[10), E. Ryabov[2), V. Samoliga[2), I. Satyshev[3), A. Silaev[1), A. Silaev (junior)[1), A. Sidorenkov[10), A. Skurikhin[1), A. Sokolov[7),6), L. Sveshnikova[1), V. Tabolenko[2), A. A. Tanaev[2), M. Y. Ternovoy[2), L. Tkachev[4), N. Ushakov[10), A. Vaidyanathan[6), N. V. Volkov[9), D. Voronin[10), A. Zagorodnikov[2), I. Yashin[3), and D. Zhurov[2),12)

Received March 2, 2023; revised March 2, 2023; accepted March 2, 2023

Abstract—This paper presents the results of an analysis of observations of the Crab Nebula gamma-ray source with the first two atmospheric Cherenkov telescopes of the TAIGA (Tunka Advanced Instrument for cosmic ray physics and Gamma Astronomy) astrophysical complex in the stereo mode of observations. The article analyzed observational data from 2020 to 2021. Over 36 hours of observations, a signal was obtained at a statistical significance level of 5σ and a spectrum of gamma rays was plotted in the energy range from 2 to 70 TeV. The paper describes a technique for gamma—hadron separation and reconstruction of detected gamma-rays energy.

DOI: 10.1134/S1063778823040385

[1)]Skobeltsyn Institute of Nuclear Physics, Moscow State University, Moscow, Russia.
[2)]Research Institute of Applied Physics, Irkutsk, Russia.
[3)]National Research Nuclear University MEPhI, Moscow, Russia.
[4)]Joint Institute for Nuclear Research, Dubna, Russia.
[5)]Dipartimento di Fisica, Generale Universita di Torino and INFN, Turin, Italy.
[6)]Novosibirsk State University, Novosibirsk, Russia.
[7)]Budker Institute of Nuclear Physics of Siberian Branch Russian Academy of Sciences, Novosibirsk, Russia.
[8)]Dubna University, Dubna, Russia.
[9)]Altai State University, Barnaul, Russia.
[10)]Institute for Nuclear Research of the Russian Academy of Sciences, Moscow, Troitsk, Russia.
[11)]Pushkov Institute of Terrestrial Magnetism, Ionosphere, and Radio Wave Propagation, Russian Academy of Sciences, Troitsk, Russia.
[12)]Irkutsk National Research Technical University, Irkutsk, Russia.
*E-mail: pvol4@ya.ru

1. INTRODUCTION

The TAIGA (Tunka Advanced Instrument for cosmic ray physics and Gamma Astronomy) Astrophysical Complex [1–3] is located in the Tunka Valley of the Buryatia Republic, 50 km from Lake Baikal. The complex is aimed at studying the physics of cosmic rays in the energy range from 10^{14} to 10^{18} eV and gamma-ray astronomy in the energy region above a few TeV. The physics of cosmic rays in TAIGA is studied by means of such installations as Tunka-133 [4] and Tunka-Grande [5]. Gamma-ray astronomy research is carried out using:

- TAIGA-IACT — Imaging Atmospheric Cherenkov Telescopes [2, 3];
- TAIGA-HiSCORE — an array of wide-angle Cherenkov detectors [6, 7].

TAIGA-HiSCORE consists of 120 Cherenkov detectors in an area of 1 km^2. The energy threshold of the installation is about 40 TeV. TAIGA-IACT currently includes 3 telescopes ∼300 m apart. It is planned that in the nearest future the installation will be expanded to 5 telescopes, which will increase the effective area of the detector. The energy threshold of each telescope in stand-alone mode is ∼2 TeV. The main idea of TAIGA is the simultaneous operation of HiSCORE wide-angle detectors, which are capable of reconstructing the arrival direction of events and the position of the EAS axis on the ground with high accuracy [8, 9], and atmospheric Cherenkov telescopes (IACTs), capable of performing gamma–hadron separation with high reliability. Such a hybrid approach makes it possible to detect gamma rays in the energy region above 100 TeV, the nature of which is currently a debatable issue, and new observational data on gamma-ray sources can clarify it. This work is focused on the study of data from the joint work of first two IACTs on TAIGA, the energy threshold of which is 8 TeV and allows the detection of bright sources of high-energy gamma rays, such as the Crab Nebula [10].

2. TAIGA-IACT

In the classification of CTA [11], TAIGA-IACTs are small size telescopes (SST). The dish of each of them follows the Davis–Cotton design and consists of 34 spherical mirrors with diameter 60 cm (9.6 m^2 total area) and the focal length of the telescopes is 4.75 m. The dish diameter is 4.3 m. The telescope's cameras contain ∼600 XP1911 PMTs grouped into clusters controlled by the MAROC3 chip. The telescope trigger is formed when the amplitude exceeds 10 photoelectrons (p.e.) in two neighboring pixels within 15 ns. The camera's field of view (FoV) is 9.6 degrees (0.36 degrees per pixel) with a 0.07 degree point spread function [7]. More technical details can be found in [12].

Based on the observational data from the first TAIGA-IACT, a signal with a statistical significance of 12σ was obtained from the gamma-ray sources Crab Nebula [13, 14] and with 5σ from the blazar MRK421 [13].

3. MONTE CARLO SIMULATION

Simulation of EAS was carried out in CORSIKA [15] version 7.35 with QGSJET-II-04 [16] model for high-energy interactions and GHEISHA-2002d [17] for low-energy interactions. EAS were modeled in the range of zenith angles of 30–40 degrees, which corresponds to the experimental observation angles of the Crab Nebula in the Tunka Valley. Gamma rays were simulated in the range from 20 to 200 TeV and protons from 40 to 400 TeV in the amount of 2.5×10^4 and 18.6×10^4, respectively. EAS axes are randomly generated over an area of 3 km^2 around the installation.

The photon bunches at the output of CORSIKA were traced in a special optical simulation program [18]. This program models the optical properties of IACT up to the PMT photocathodes and outputs individual photoelectrons to the IACT camera. After that, each photoelectron is passed through the telescope's trigger simulation program. The photoelectron amplitudes are chosen randomly, in accordance with the experimentally measured amplitude distribution of the XP1911 PMT in [19], where the effect of afterpulses is also taken into account. As a result, an EAS image is formed in the camera of each telescope, the analysis of which makes it possible to estimate the energy and type of particles (hadron/gamma).

4. MONTE CARLO CALCULATIONS OF THE TELESCOPE RESPONSE AND THEIR EXPERIMENTAL CALIBRATION

For a correct reconstruction of the parameters of primary particles, it is necessary to know the ratio between the total number of photoelectrons recorded by telescopes ($size$) and the flux of Cherenkov photons generated in EAS reaching IACT (Q). To calculate the coupling coefficient $R = size/Q$, events detected by the TAIGA-IACT01 and the TAIGA-HiSCORE installation were selected. For these events, according to the data of the HiSCORE detectors, lateral distribution functions (LDFs) were constructed, on the basis of which the flux of Cherenkov photons at the telescope location was determined. The distribution of $R_{\rm exp}$ is shown in Fig. 1. The average value of this is $0.56 \pm 0.03 \pm 0.07_{\rm syst}$. A similar coefficient included in the simulation is $R_{\rm sim} = 0.63 \pm 0.03$, which, within the limits of the error, agrees with the experimentally measured value.

5. RECONSTRUCTION OF EAS PARAMETERS

Events with the following parameters were selected for reconstruction:

- a total number of p.e. above 120;
- dist0[13] <3.5 degrees;

[13] dist0 is the angle between the direction of the maximum shower development (the image CoG) and the direction of the telescope.

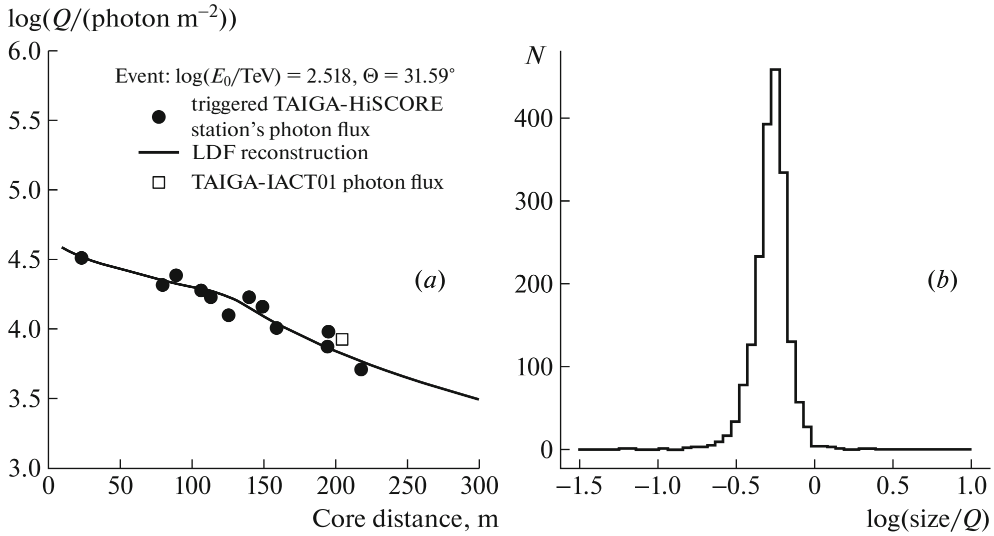

Fig. 1. (*a*) An example of the EAS spatial distribution function; (*b*) experimental distribution of the coefficient R.

- events detected by the both telescopes.

For these events parameters such as the EAS arrival direction in the FoV of the telescope camera, the position of the shower axis on the ground (*impact parameter*), and the shower development maximum ($X_{\max}$) were reconstructed.

The particle arrival direction was determined as the weighted average position of the intersection points of the main axes of the EAS images in each IACT camera. This procedure has been described in detail in [10]. The accuracy of arrival direction reconstruction for the first two IACTs is 0.25 degrees. Here and below, the reconstruction accuracy means the size of the region within which 68% of the events from the number of events included in the analysis are contained.

For reconstruction of an EAS core position, a similar technique is used. In this case, the positions of the telescopes relative to each other, as well as the zenith angle of observation, are taken into account. In addition, since the position of the observed source in camera is known, lines connecting the CoGs of the event with this position are used instead of crossing the main image axes. The accuracy of axis location determination for the first two IACTs was found to be equal to 18 meters.

The $X_{\max}$ parameter can be reconstructed if the height of the shower development maximum is known. The shower development maximum corresponds to the image CoG, and at a known distance to the EAS axis, the height of the shower development maximum can be calculated from geometric considerations [20]:

$$\text{height} = \frac{\text{impact parameter}}{\text{dist1}}, \tag{1}$$

where dist1 is the angle between the EAS arrival direction and the image CoG. Altitude can be converted to g/cm^2 using the Standard Atmosphere Model for an altitude of 450 m above sea level and an average temperature of $-17.5°$C [21].

6. GAMMA–HADRON SEPARATION

The main parameters of events for gamma–hadron separation are *normalized width* and θ^2. θ is the angle between the direction to the EAS source and the reconstructed shower arrival direction. The *normalized width* is the sum of the *widths* of the EAS images in each triggered IACT, normalized to the distance to the EAS axis and the number of triggered telescopes. A detailed description of the *normalized width* can be found in [10, 22].

The criteria for gamma selection were found through optimization, in which a cut was applied to each of these two parameters, the value of which varied from the minimum possible value of this parameter to the maximum. Such a combination of selection criteria was found, in which the fraction of stored gamma rays remains at the level of 50% of the number of events recorded in the stereo mode, and the hadron suppression is maximum. The resulting hadron suppression was $\sim 3.8 \times 10^{-5}$. The effective area for gamma rays was obtained as 0.2 km^2 in the energy region above 60 TeV (Fig. 2).

7. DETECTION OF THE GAMMA RAYS FROM THE CRAB NEBULA

The analysis of observations of the gamma ray source Crab Nebula included 37 hours of observation

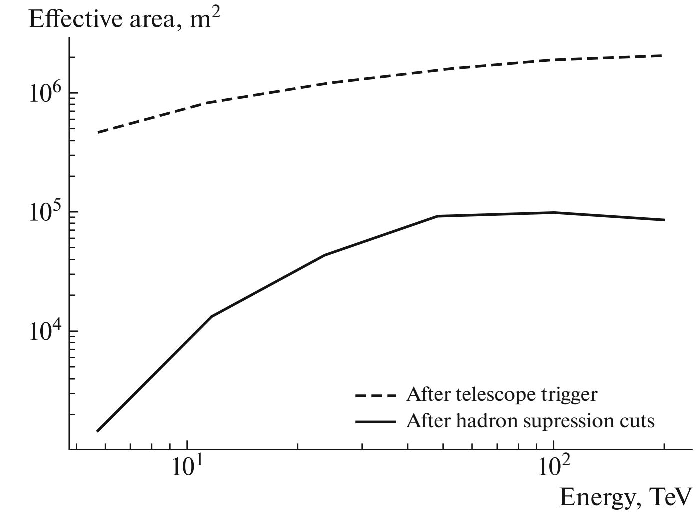

Fig. 2. Effective area TAIGA-IACT in stereo mode with first two telescopes.

from October 2020 to February 2021. The experiment uses the wobble observation technique [23]: the telescope is directed in such a way that the source is at a distance of 1.2 degrees from the center of the camera every 20 minutes. This approach makes it possible to eliminate the influence of the features of individual camera pixels on the resulting excess of gamma rays. To increase the statistical significance of the gamma-ray excess, the background was estimated from 7 background regions in the camera's FoV, 1.2 degrees away from the camera center.

As a result of applying the optimal selection criteria obtained in the simulation to the events detected in the experiment, an excess of 37 gamma-like events from the region containing the source in relation to 7 background regions was obtained. The significance of the excess was calculated based on the Li–Ma equation [24] and amounted to 5σ (Fig. 3).

8. ENERGY RECONSTRUCTION

For energy reconstruction of gamma rays, the dependence of the energy on *size* in the image detected by the telescope in the simulation was determined for different values of $X_{\max}$ and *impact parameters*. In this regard, the entire space of possible $X_{\max}$ and *impact parameters* was divided into separate bins with a step of 70 g/cm^2 and 10 m, respectively. For events that fell into a certain bin by $X_{\max}$ and *impact parameters*, linear dependences of energy on *size* were determined, on the basis of which the reconstructed energy can be obtained. For this method the energy resolution is 10% for a range from 20 to 200 TeV.

The energy of 37 gamma-like events selected in the experiment was determined using this method, as a result of which the spectrum of gamma rays was plotted in the energy region above 5 TeV. The spectrum is in good agreement with the measurements of other gamma-ray observatories (Fig. 4). The last bin of the spectrum in the range from 34 to 69 TeV contains 6 gamma-like events.

9. CONCLUSIONS

This paper presents a method for reconstructing EAS parameters from primary gamma rays recorded by the first two atmospheric Cherenkov telescopes of the TAIGA astrophysical complex in stereo mode.

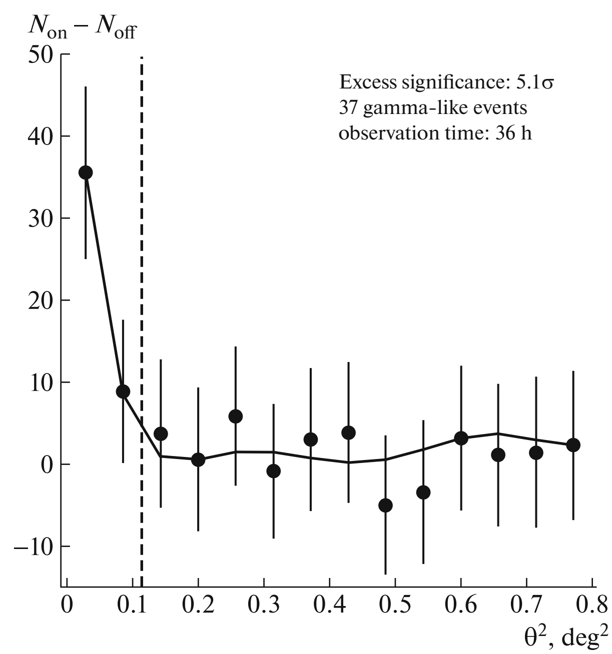

Fig. 3. θ^2 distribution for gamma-like events.

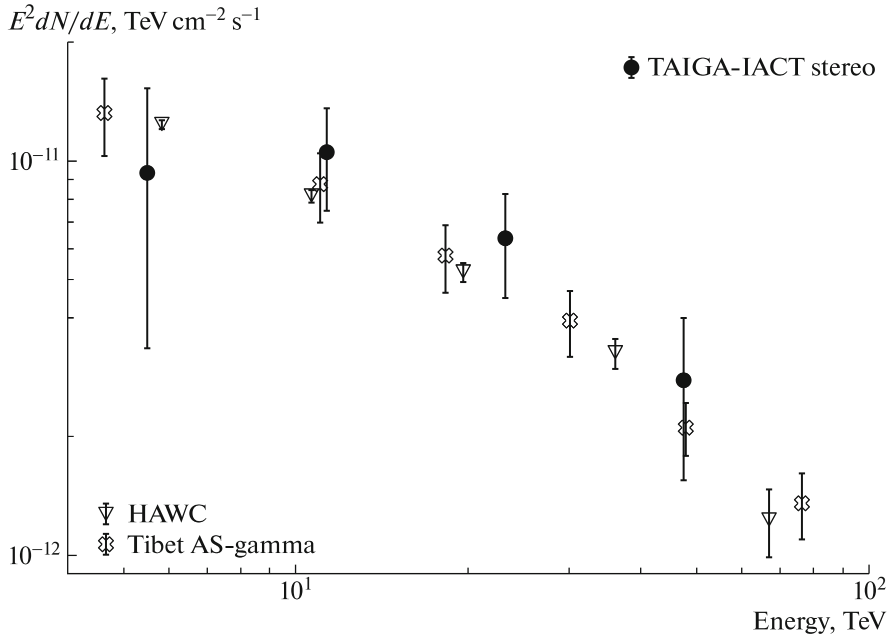

Fig. 4. Energy spectrum of gamma rays from the Crab Nebula measured by the first two IACTs in TAIGA in stereo mode. The last bin of the spectrum in the range from 34 to 69 TeV contains 6 gamma-like events.

Based on these parameters, gamma–hadron separation and reconstruction of the energy spectrum of selected gamma rays from the Crab Nebula was carried out. The obtained spectrum from 5 to 69 TeV is in good agreement with the observations of other observatories. With the TAIGA-IACT03, we expect to detect 30–40 gamma rays from the Crab Nebula in 300 hours with energies above 100 TeV, which will be an important result for Cherenkov measurements, since at present gamma rays with similar energies are detected only by high-mountain installations detecting charged EAS particles.

ACKNOWLEDGMENTS

The work was performed at the UNU "Astrophysical Complex of MSU-ISU" (agreement EB-075-15-2021-675). The work is supported the Russian Federation Ministry of Science and High Education (projects FZZE-2020-0024 and FZZE-2023-0004) and by Russian Foundation for Basic Research, grant 23-72-00019 (Sections 3–6, 23-72-00016).

REFERENCES

1. L. A. Kuzmichev, I. I. Astapov, P. A. Bezyazeekov, V. Boreyko, A. N. Borodin, N. M. Budnev, R. Wischnewski, A. Y. Garmash, A. R. Gafarov, N. V. Gorbunov, V. M. Grebenyuk, O. A. Gress, T. I. Gress, A. A. Grinyuk, O. G. Grishin, A. N. Dyachok, et al., Phys. At. Nucl. **81**, 4 (2018).
2. N. Budnev, I. Astapov, P. Bezyazeekov, E. Bonvech, V. Boreyko, A. Borodin, M. Bruckner, A. Bulan, D. Chernov, D. Chernykh, A. Chiavassa, A. Dyachok, O. Fedorov, A. Gafarov, A. Garmash, V. Grebenyuk, et al., J. Instrum. **15**, C09031 (2020).
3. N. Budnev, I. Astapov, P. Bezyazeekov, E. Bonvech, A. Borodin, M. Brückner, A. Bulan, D. Chernov, A. Chiavassa, A. Dyachok, A. Gafarov, A. Garmash, V. Grebenyuk, O. Gress, T. Gress, A. Grinyuk, et al., Phys. At. Nucl. **84**, 362 (2021).
4. S. Berezhnev, D. Besson, N. Budnev, A. Chiavassa, O. Chvalaev, O. Gress, A. Dyachok, S. Epimakhov, A. Haungs, N. Karpov, N. Kalmykov, E. Konstantinov, A. Korobchenko, E. Korosteleva, V. Kozhin, L. Kuzmichev, et al., Nucl. Instrum. Methods Phys. Res., Sect. A **692**, 98 (2012).
5. R. Monkhoev, N. Budnev, A. Chiavassa, A. Dyachok, A. Gafarov, O. Gress, T. Gress, O. Grishin, A. Ivanova, N. Kalmykov, Y. Kazarina, E. Korosteleva, V. Kozhin, L. Kuzmichev, V. Lenok, B. Lubsandorzhiev, et al., J. Instrum. **12**, C06019 (2017).
6. M. Tluczykont, D. Hampf, D. Horns, D. Spitschan, L. Kuzmichev, V. Prosin, C. Spiering, and R. Wischnewski, Astropart. Phys. **56**, 42 (2014).
7. L. Kuzmichev, I. Astapov, P. Bezyazeekov, A. Borodin, M. Brückner, N. Budnev, A. Chiavassa, O. Gress, T. Gress, O. Grishin, A. Dyachok, O. Fedorov, A. Gafarov, A. Garmash, V. Grebenyuk, A. Grinyuk, et al., Nucl. Instrum. Methods Phys. Res., Sect. A **952**, 161830 (2020).
8. L. Kuzmichev, I. Astapov, P. Bezyazeekov, V. Boreyko, A. Borodin, M. Brückner, N. Budnev, A. Chiavassa, O. Gress, T. Gress, O. Grishin, A. Dyachok, S. Epi-

makhov, O. Fedorov, A. Gafarov, V. Grebenyuk, et al., EPJ Web Conf. **145**, 01001 (2017).

9. M. Tluczykont, N. Budnev, I. Astapov, N. Barbashina, A. Bogdanov, V. Boreyko, M. Bruckner, A. Chiavassa, O. Chvalaev, O. Gress, T. Gress, O. Grishin, A. Dyachok, S. Epimakhov, O. Fedorov, A. Gafarov, et al., EPJ Web Conf. **136**, 03008 (2017).
10. A. Grinyuk, E. Postnikov, P. Volchugov, I. Astapov, A. Awad, P. Bezyazeekov, M. Blank, A. Borodin, A. Bulan, M. Brueckner, N. Budnev, A. Chiavassa, A. Dyachok, O. Gress, T. Gress, O. Grishin, et al., PoS (ICRC2021) 395 (2021).
11. M. Actis, G. Agnetta, F. Aharonian, A. Akhperjanian, J. Aleksić, E. Aliu, D. Allan, I. Allekotte, F. Antico, L. A. Antonelli, P. Antoranz, A. Aravantinos, T. Arlen, H. Arnaldi, S. Artmann, K. Asano, et al., Exp. Astron. **32**, 193 (2011).
12. N. Lubsandorzhiev, I. Astapov, P. Bezyazeekov, V. Boreyko, A. Borodin, M. Brueckner, N. Budnev, A. Chiavassa, A. Dyachok, O. Fedorov, A. Gafarov, A. Garmash, N. Gorbunov, V. Grebenyuk, O. Gress, T. Gress, et al., PoS (ICRC2017) F135186 (2017).
13. L. Sveshnikova, I. Astapov, P. Bezyazeekov, M. Blank, A. Borodin, M. Brucknerr, N. Budnev, A. Bulan, A. Vaidyanathan, R. Wischnewski, P. Volchugov, D. Voronin, A. Gafarov, A. Garmash, V. Grebenyuk, O. Gress, et al., Bull. Russ. Acad. Sci.: Phys. **85**, 398 (2021).
14. L. Sveshnikova, P. Volchugov, E. Postnikov, I. Astapov, P. Bezyazeekov, E. Bonvech, A. Borodin, N. Budnev, A. Bulan, A. Vaidyanathan, N. Volkov, D. Voronin, A. Gafarov, E. Gress, O. Gress, T. Gress, et al., in *Proceedings of the 37th Russian Cosmic Ray Conference* (Moscow, 2022).
15. D. Heck, J. Knapp, J. N. Capdevielle, G. Schatz, and T. Thouw, Tech. Rep. FZKA-6019 (Forschungszentrum Karlsruhe, 1998).
16. S. Ostapchenko, Phys. Rev. D **83**, 014018 (2011).
17. H. Fesefeldt, Tech. Rep. (Phys. Inst., Tech. Hochschule Aachen (PITHA), Aachen, 1985).
18. A. Grinyuk, E. Postnikov, and L. Sveshnikova, Phys. At. Nucl. **83**, 262 (2020).
19. R. Mirzoyan, E. Lorenz, D. Petry, and C. Prosch, Nucl. Instrum. Methods Phys. Res., Sect. A **387**, 74 (1997).
20. W. Hofmann, H. Lampeitl, A. Konopelko, and H. Krawczynski, Astropart. Phys. **12**, 207 (2000).
21. V. Prosin, Doctoral Dissertation (SINP MSU, Moscow, 2006).
22. H. Krawczynski, D. A. Carter-Lewis, C. Duke, J. Holder, G. Maier, S. Le Bohec, and G. Sembroski, Astropart. Phys. **25**, 380 (2006).
23. V. P. Fomin, A. A. Stepanian, R. C. Lamb, D. A. Lewis, M. Punch, and T. C. Weekes, Astropart. Phys. **2**, 137 (1994).
24. T.-P. Li and Y.-Q. Ma, Astrophys. J. **272**, 317 (1983).